Adv Syst Sci Appl 2024; **03**; 43-57
Published online at https://ijassa.ipu.ru.

Enhancing Comfort and Stability of a Vehicle Suspension System when Oscillating by an Optimal Hybrid Control Algorithm

Tuan Anh Nguyen*

Thuyloi University, Hanoi, Vietnam

Abstract: This article proposes a control algorithm for an automotive suspension system to improve ride comfort. The control method is based on the combination of Sliding Mode Control (SMC) and Proportional-Integral-Derivative (PID), with parameters optimally selected by an in-loop algorithm called OSMCPID. The system's performance is evaluated by simulation, which goes through three specific cases. According to the article's findings, in the first two cases, the average value of vehicle body displacement when using the proposed algorithm is only 7.71% and 6.96%, respectively, compared to mechanical suspension. In the third case, vehicle body displacement approaches zero once the road excitation signal ends. Meanwhile, the remaining cases have a more significant gap. In addition, the phase difference of the control signal is slight, while the chattering phenomenon almost does not occur when using the hybrid algorithm. In general, the system can adapt to changing external conditions.

Keywords: Active suspension system, hybrid algorithm, chattering phenomenon, vehicle vibration.

1. INTRODUCTION

Roughness on the road might cause the automobile to oscillate while it is in motion. This will cause passengers to feel very uncomfortable. Additionally, the quality of the merchandise is also impacted. There are several criteria used to assess vehicle oscillations. Commonly employed metrics include the change in the sprung mass displacement, acceleration, and the oscillation phase differential. The maximum values of the above criteria should be considered for a single impulse or discontinuous oscillations. Their mean data will be evaluated regarding continuous or periodic oscillations.

A suspension system is used to control the automobile's oscillations. Each type of suspension system will have a variety of components. A passive suspension system uses a metal spring and conventional damper. The overall stiffness of these elements has not changed. Therefore, the vehicle's smoothness cannot be guaranteed. The spring and damper stiffness must be altered to eliminate the vehicle's oscillation problems. In [1], Marenkov and Baurova presented the air suspension mechanism. This suspension has variable-stiffness air springs. Internal pneumatic pressure variations alter the spring's stiffness [2, 3]. In addition, the suspension system employing a magnetorheological damper helps increase the vehicle's movement stability. The magnetorheological damper utilizes electromagnetic force to control the movement of liquid inside [4]. The oscillation quenching procedure can thus be adjusted easily [5]. Active suspension technologies should be employed widely to improve oscillation [6, 7]. For each position of the active suspension, there is an extra hydraulic actuator. This actuator's operation depends on the movement of inside hydraulic valves [8]. These valves work once control signals from the controller is received [9]. In general, an active suspension system's performance can be more fantastic than other suspension systems.

* Corresponding author: anhngtu@tlu.edu.vn

For fundamental control issues, the linearity of the object is frequently assumed. The PID algorithm may be implemented if the controlled object has only one input and one output, also known as the Single Input and Single Output (SISO) system. The PID controller has three distinct phases. There will be a matching coefficient for each step [10]. The selection of optimal parameters for this controller is essential. In [11], Han et al. presented a method for adjusting the PID controller's coefficients based on fuzzy principles. In another study, Demir et al. used fuzzy method to tune these factors [12]. The fuzzy algorithm described in [12] had two inputs and one output. The defuzzification procedure was created from the perspective of the designer. The membership functions of fuzzy algorithms were commonly trapezoidal or triangular [13]. In certain instances, a Gaussian functional form might be utilized [14]. The fuzzy technique could make factors of the PID controller change continuously. This was an effective adaptive response [15]. Furthermore, particle swarm optimization approaches might optimize PID controller configurations [16-19]. When controlling both displacement and acceleration, two PID controllers could be coordinated [20]. However, this might result in undesirable interactions [21]. In [22], Nguyen et al. controlled active suspension with the quarter-dynamics model using the Linear Quadratic Regulator (LQR) method. This algorithm was often applied to Multi-Input and Multi-Output (MIMO) systems. This approach was designed to minimize the cost function [23]. In order to efficiently solve the Riccati algebraic equation, every oscillation state model of the automobile must be expressed in the form of a state matrix [24]. When this controller had incorporated the "cancellation term" further, it was referred to as i-LQR. Haddar presented this concept in [25].

The SMC technique was frequently applied to individuals with random or nonlinear stimuli [26]. This approach employed Lyapunov theory to create asymptotically stable controllers [27]. According to Nguyen [28], every controlled object would travel across the sliding surface until a steady state was reached. The sliding surface was built according to the model's high-order derivative signal [29]. Therefore, the actuator must be linearized into an approximation of a linear differential equation. This procedure was established in [30] by Nguyen et al. The order of the signal's derivative would depend on the system's order. The control model got more complicated if a system had many more state variables [31]. Using the SMC algorithm frequently resulted in the “chattering” effect. There might be a disturbance in the control signals [32-34]. Combining the SMC algorithm with the fuzzy or PID algorithm could help solve this problem. Then, the system's controller would be referred to as a “hybrid control” [35, 36]. In addition, several more complex control algorithms [37-39] were employed to regulate the performance of an active suspension system. Overall, these strategies were also exceptionally practical.

An optimal algorithm (OSMCPID) is proposed in this work to control the suspension system to limit the influence of chattering and suppress the system error. Two control signals are used to synthesize the ultimate controller's control signal. The controller's parameters are optimally selected by the in-loop algorithm. The integration method will depend on the researchers' design perspective. This article is divided into four sections: Introduction, Models, Simulation and result, and Conclusion.

2. MODELS

In this work, a model of the quarter-dynamic is utilized in order to simplify the modelling of vehicle oscillation (Figure 2.1). This dynamic model incorporates both two mass, and the suspension system containing the conventional spring and damping connects them. The hydraulic actuator is installed with a suspension system to enhance ride comfort. Consequently, a mechanical suspension system (passive) develops into an electronic suspension system (active).

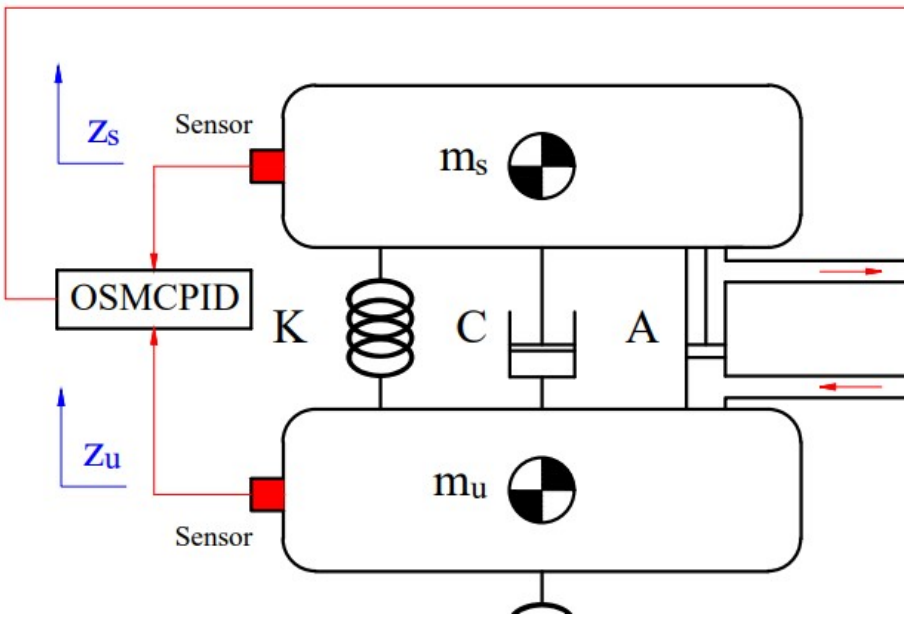

Figure 2.1. Automobile dynamic model.

An automobile's dynamic model has two degrees of freedom for each direction of movement, including z_s and z_u. Using mechanic theory, equations (2.1) and (2.2) describe vehicle oscillations.

$$m_s\ddot{z}_s = K\left(z_u - z_s\right) + C\left(\dot{z}_u - \dot{z}_s\right) + F_A \tag{2.1}$$

$$m_u\ddot{z}_u = K_T\left(z_r - z_u\right) - K\left(z_u - z_s\right) - C\left(\dot{z}_u - \dot{z}_s\right) - F_A \tag{2.2}$$

where m_s and m_u are sprung mass and unsprung mass, respectively; z_s and z_u are sprung mass displacement and unsprung displacement, respectively; K is the suspension spring coefficient; C is the suspension damper coefficient; and K_T is the tire spring coefficient.

In order to decrease the oscillation of an automobile, a hydraulic actuator should provide an impact force. This force impacts the sprung and unsprung masses. The actuator force (F_A) is created by the pressure difference between the two compartments within the actuator. This force's magnitude is proportional to the piston's area, S_p, and the pressure differential, ΔP, according to (2.3).

$$F_A = S_p\Delta P \tag{2.3}$$

The actuator work thanks to the voltage signal provided by the controller. The internal valves will travel when the voltage signal is delivered to the hydraulic actuator. This movement changes the pressure of the fluid within the cylinder. A complicated multivariable function was used to describe a dependence between the control signal, $u(t)$, the displacement of valves, x_{sv}, and the pressure difference. Even the suspension system displacement, x_s, is a factor. This dependence is demonstrated by equations (2.4) and (2.5).

$$x_{sv} = \frac{1}{\tau}\int\left(k_{sv}u\left(t\right) - x_{sv}\right)dt \tag{2.4}$$

$$\Delta P = \rho_3\int\left(x_{sv}\sqrt{P_s - sgn\left(x_{sv}\right)\Delta P}\right)dt - \rho_2\int\Delta P dt - \rho_1 S_p\int\dot{x}_s dt \tag{2.5}$$

Using the original hydraulic actuator equations makes the design of the controller extremely challenging. According to [30], the impact force, F_A, produced by an actuator may be linearized as (2.6), where ξ_i are coefficients.

$$\dot{F}_A = \xi_1 u\left(t\right) - \xi_2 F_A - \xi_3\left(\dot{z}_s - \dot{z}_u\right) \tag{2.6}$$

According to [28], sprung mass' acceleration may be estimated as (2.7), where χ is a coefficient.

$$\ddot{z}_s = \frac{K_T}{\chi m_s}\left(z_r - z_u\right) \tag{2.7}$$

Let state variables:

$$x_1 = z_s \qquad x_2 = \dot{z}_s \qquad x_3 = z_u \qquad x_4 = \dot{z}_u \qquad x_5 = F_A$$

Taking derivatives of state variables, we get (2.8) to (2.12).

$$\dot{x}_1 = x_2 \tag{2.8}$$

$$\dot{x}_2 = \frac{1}{m_s}\left(-Kx_1 - Cx_2 + Kx_3 + Cx_4 + x_5\right) \tag{2.9}$$

$$\dot{x}_3 = x_4 \tag{2.10}$$

$$\dot{x}_4 = \frac{1}{m_u}\left(Kx_1 + Cx_2 - \left(K + K_T\right)x_3 - Cx_4 - x_5\right) \tag{2.11}$$

$$\dot{x}_5 = \xi_1 u\left(t\right) - \xi_3 x_2 + \xi_3 x_4 - \xi_2 x_5 \tag{2.12}$$

Let $e_1(t)$ be the error of two signals, include the output signal and the setpoint signal of the sliding mode controller.

$$e_1\left(t\right) = y_{s1}\left(t\right) - y\left(t\right) \tag{2.13}$$

Take the derivative of both sides of (2.13), we obtain (2.14).

$$\dot{e}_1\left(t\right) = \dot{y}_s\left(t\right) - \dot{y}\left(t\right) = \dot{y}_s\left(t\right) - x_2 \tag{2.14}$$

The second derivative of the equation (2.13) is shown in (2.15).

$$\ddot{e}_1\left(t\right) = \ddot{y}_s\left(t\right) - \ddot{y}\left(t\right) = \ddot{y}_s\left(t\right) - \frac{K_T}{\chi m_s}\left(x_3 - z_r\right) \tag{2.15}$$

Take the derivative of both sides of (2.15), we get (2.16).

$$e_1^{(3)}\left(t\right) = y_s^{(3)}\left(t\right) - y^{(3)}\left(t\right) = y_s^{(3)}\left(t\right) - \frac{K_T}{\chi m_s}\left(x_4 - \dot{z}_r\right) \tag{2.16}$$

By continuing to derive both sides of (2.16), we can obtain (2.17).

$$\begin{aligned} e_1^{(4)}\left(t\right) &= y_s^{(4)}\left(t\right) - y^{(4)}\left(t\right) \\ &= y_s^{(4)}\left(t\right) + \frac{K_T}{\chi m_s m_u}\left(Kx_1 + Cx_2 - \left(K + K_T\right)x_3 - Cx_4 - x_5\right) - \frac{K_T}{\chi m_s}\ddot{z}_r \end{aligned} \tag{2.17}$$

Let's use the symbols as (2.18–2.23):

$$\theta_1 = KC\left(\frac{1}{m_s} + \frac{1}{m_u}\right) \tag{2.18}$$

$$\theta_2 = \left(\frac{C^2}{m_s} + \frac{C^2}{m_u} - K - \xi_3\right) \tag{2.19}$$

$$\theta_3 = -C\left(\frac{K}{m_s} + \frac{K + K_T}{m_u}\right) \tag{2.20}$$

$$\theta_4 = -\left(\frac{C^2}{m_s} + \frac{C^2}{m_u} - K - K_T - \xi_3\right) \tag{2.21}$$

$$\theta_5 = -\left(\frac{C}{m_s} + \frac{C}{m_u} + \xi_2\right) \tag{2.22}$$

$$\theta_6 = \frac{K_T \xi_1}{\chi m_s m_u} \tag{2.23}$$

The effect of systematic noise $r(t)$ is ignored. The fifth derivative signal of the output is written according to (2.24).

$$y^{(5)}(t) = \theta_1 x_1 + \theta_2 x_2 + \theta_3 x_3 + \theta_4 x_4 + \theta_5 x_5 + \theta_6 i(t) \tag{2.24}$$

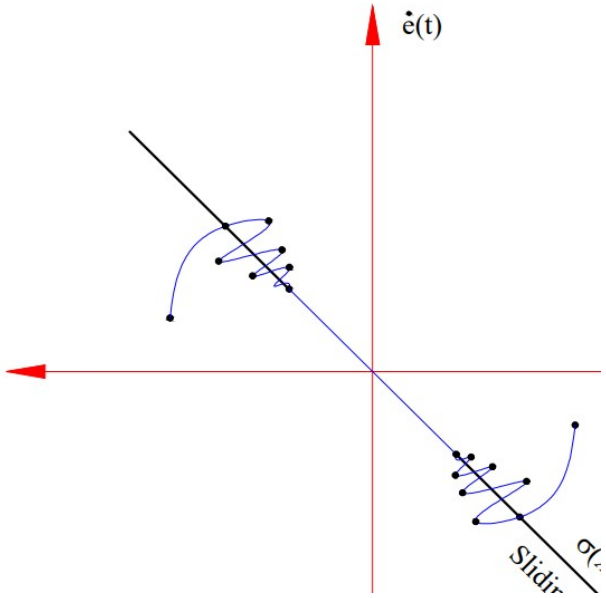

Figure 2.2. Sliding surface.

Following the Lyapunov theory, a controlled object will return to a state of equilibrium by sliding down the surface (Figure 2.2). Therefore, the sliding surface must be selected according to the system's stability requirement. A sliding surface (2.25) is the function dependent on the system's error, $e_1(t)$:

$$\sigma = \sum_{i=1}^{n} \sum_{j=0}^{n-1} \theta_j e_1^{(n-i)}(t) \tag{2.25}$$

Once a sliding surface has been established, it is simple to calculate output signals of the sliding mode controller using an equation (2.26).

$$u_1(t) = \theta_6^{-1} \left[y_s^{(n)}(t) - \sum_{k=1}^{n} \theta_k x_k(t) + \sum_{i=1}^{n} \sum_{j=0}^{n-1} \theta_j e_1^{(n-i)}(t) + J \operatorname{sgn}\left(\sum_{m=0}^{n-1} \sum_{l=0}^{n-1} \theta_m e_1^{(n-1-l)}(t) \right) \right] \tag{2.26}$$

A Lyapunov control function is chosen according to (2.27). Taking the derivative of (2.27), we obtain (2.28).

$$V(x) = \frac{1}{2}\sigma^2 > 0 \forall x \neq 0 \tag{2.27}$$

$$\dot{V}(x) = \sigma\dot{\sigma} \tag{2.28}$$

Take the derivative of the sliding surface (2.25). Then, substituting the result just found and the control signal $u_1(t)$ mentioned in (2.26) into (2.28), we obtain (2.29).

$$\dot{V}(x) = -J\sigma \operatorname{sgn}(\sigma) < 0 \tag{2.29}$$

Let $e_2(t)$ be the error of a PID controller, as (2.30).

$$e_2(t) = y_{s2}(t) - y(t) \tag{2.30}$$

A control signal, $u_2(t)$, is calculated using the following formula (2.31):

$$u_2(t) = K_P e_2(t) + K_I \int_0^t e_2(\tau) d\tau + K_D \frac{de_2(t)}{dt} \tag{2.31}$$

Using the in-loop algorithm, the PID and SMC controller's parameters are optimally chosen to increase the system's responsiveness to changing external inputs. The schemata of the control algorithm are shown in Figure 2.3. This algorithm is established found some of the following points of view:

- Peak value and mean value of a vehicle body displacement are minimum

- Peak value and mean value of a vehicle body acceleration are minimum
- The phase difference of oscillation is minimum
- Chattering phenomenon must not exist

The integrated controller's common control signal is determined by the control signals of two distinct controllers. The process of calculation and simulation will be implemented as soon as the controller has been fully designed.

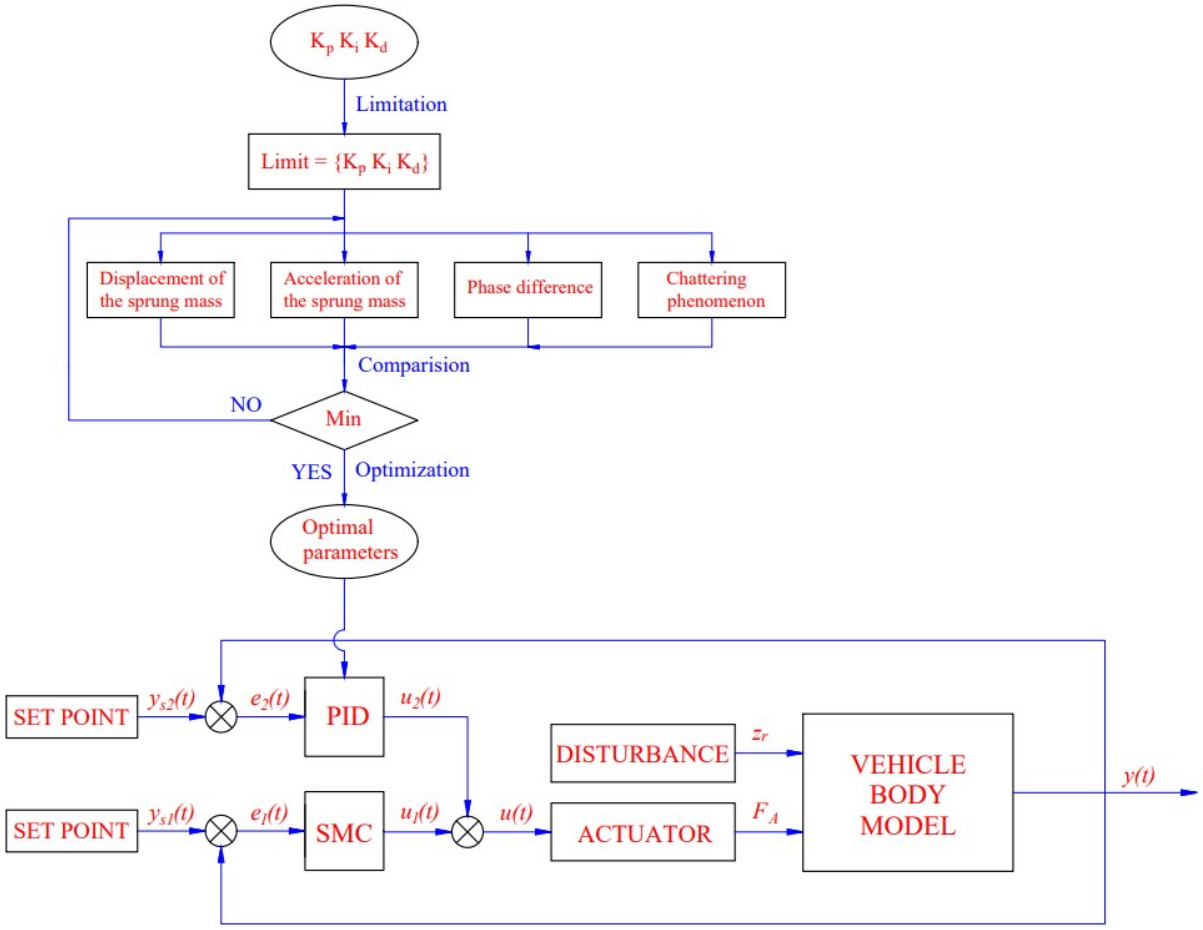

Figure 2.3. Control system diagram.

3. SIMULATION AND RESULT

3.1. Simulation

The numerical simulation method was used for this research. In this article, MATLAB-Simulink software is used. Three cases are investigated corresponding to the three types of input stimulus signals (Figure 3.1). Input stimulus signals are the bumpy road surface. The output of a simulation problem can include displacement values and acceleration values of an automotive body. In each case, four situations are considered, including:

- An automobile utilizing the active suspension system controlled by a novel hybrid method (OSMCPID) – The first situation.
- An automobile utilizing the active suspension system controlled by the SMC method – The second situation.
- An automobile utilizing the active suspension system controlled by the PID method – The third situation.
- An automobile utilizing the passive suspension system (None) – The fourth situation.

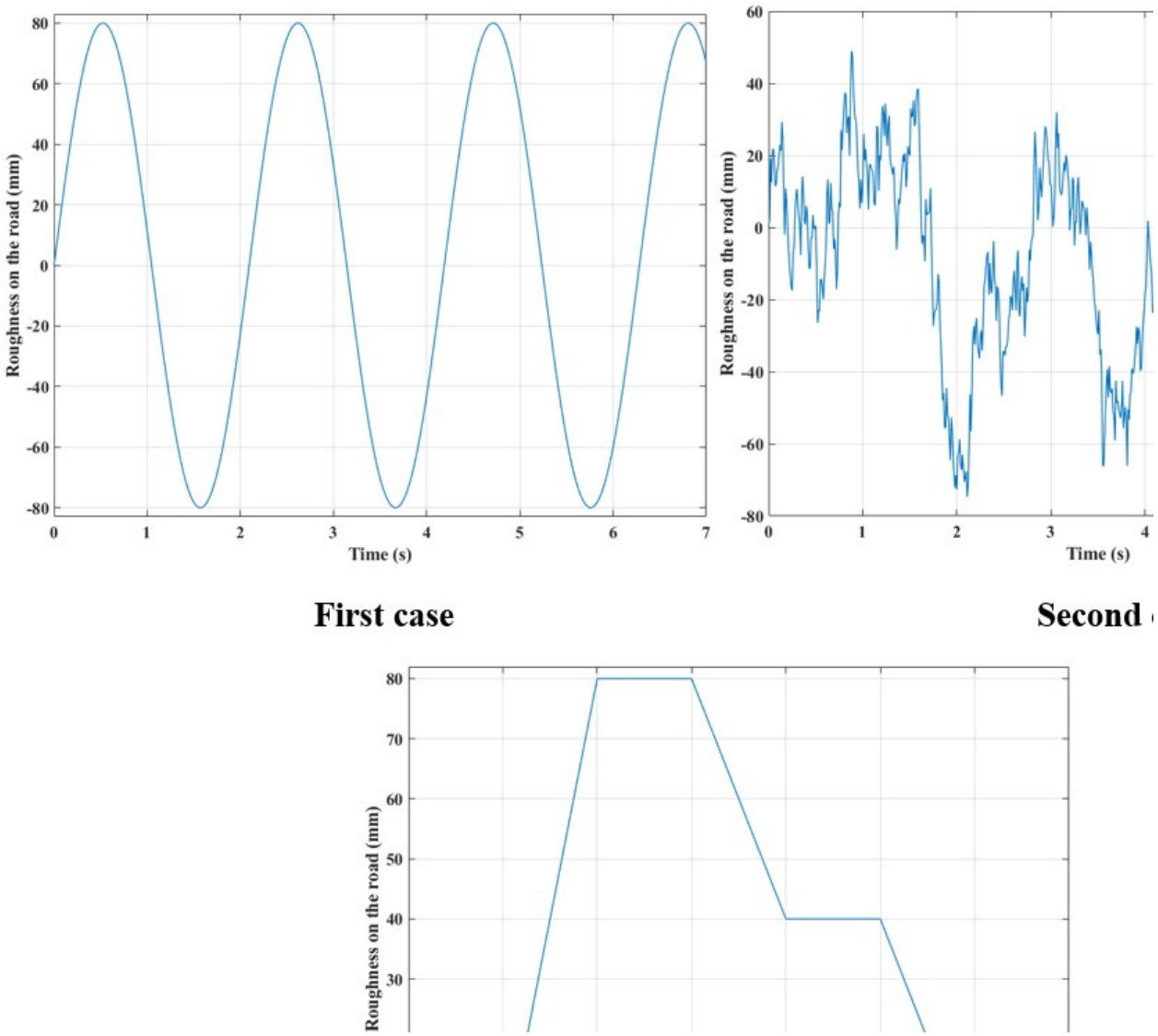

Figure 3.1. The roughness of the road surface.

The specifications of a reference automobile are shown in Table 3.1.

Table 3.1. The reference vehicle.

Description	Symbol	Unit	Value
Sprung mass	m_s	kg	470
Unsprung mass	m_u	kg	42
Tire coefficient	K_T	Nm^{-1}	177000
Spring coefficient	K	Nm^{-1}	39500
Damping coefficient	C	Nsm^{-1}	3150

3.2. Results and Discussion

Simulation results are discussed in three specific cases. The stimulus amplitude in all three cases is $r(t)$ = 80 mm. However, the frequency and acceleration of the oscillation are different.

The first case:

Sine-shaped stimulus is used for the first case. This is a low-frequency excitation. The trajectory of the excitation signal varies cyclically with time. Therefore, the oscillation of the vehicle also has a cyclical form. The change in vehicle body displacement can be observed in Figure 3.2. For vehicles using only the mechanical suspension, the peak displacement value can be up to 101.00 mm. This value is reached in the first half of the first phase of the

oscillation. From the second half of the first phase onwards, a maximum amplitude of the oscillation is only 91.25 mm. The mean oscillation value determined based on the Root Mean Square (RMS) criterion is 65.36 mm. The vehicle body displacement is able to be declined once an active suspension is used instead. Once a PID controller is utilized to direct an active suspension, the displacement value is reduced to 37.30 mm and 26.50 mm, respectively, the peak and mean oscillation value. SMC controller can help reduce oscillation values more than the PID controller, only 13.84 mm and 9.78 mm. In particular, if the OSMCPID algorithm is utilized for a suspension system, the maximum value and mean value of a vehicle body displacement are significantly reduced to only 7.12 mm and 5.04 mm.

Besides assessing the magnitude of the oscillation, the phase deviation of the oscillation should also be considered. The slightest phase deviation belongs to the first situation (OSMCPID). Meanwhile, the deviation between the second (SMC) and third (PID) situations is more significant than the fourth. Therefore, the OSMCPID algorithm can provide better performance with high accuracy.

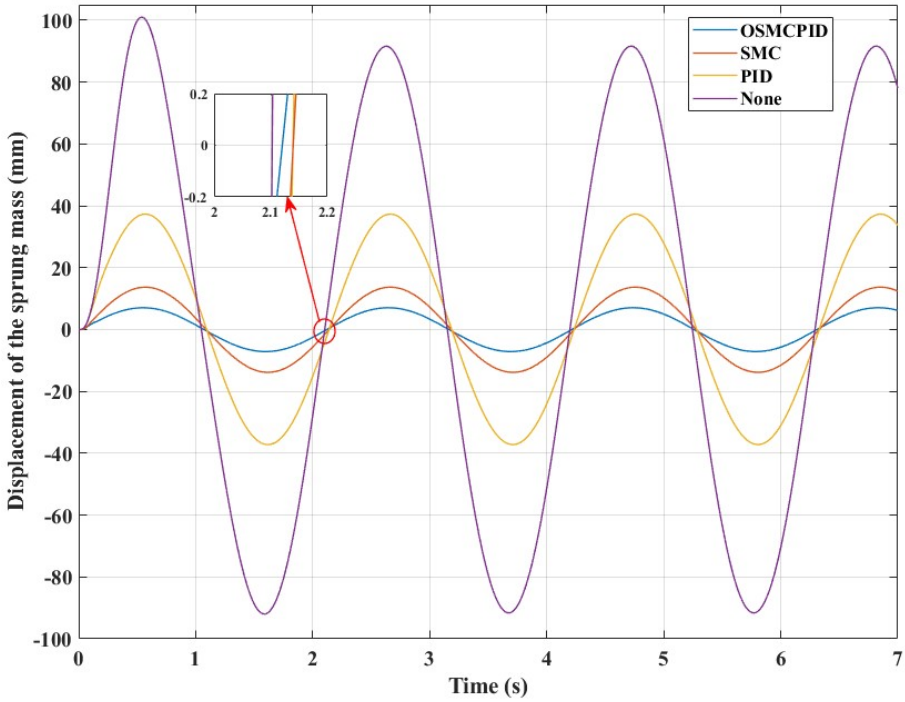

Figure 3.2. Sprung mass displacement (The first case).

A vehicle's acceleration is the value used to evaluate the smoothness of a vehicle when it oscillates. If the value of acceleration is high, there is a possibility that smoothness will be reduced. The change of acceleration throughout the simulation period is illustrated in Figure 3.3. The acceleration of the vehicle body reaches its peak value at the first phase, respectively 0.69 m/s^2, 0.91 m/s^2, 1.68 m/s^2, and 1.90 m/s^2, corresponding to the four situations examined. In the following phases, the vehicle body acceleration oscillates with a stable amplitude. The mean value of the vehicle body acceleration determined according to the RMS criterion reached 0.07 m/s^2, 0.11 m/s^2, 0.28 m/s^2, and 0.68 m/s^2, respectively. Compared with the fourth situation, the average acceleration value, once the OSMCPID algorithm is used for the suspension system, is only 10.29%. In some situations, during phase transition, the value of the acceleration may change suddenly. However, this change is quite small. Therefore, this has no impact whatsoever on how smoothly the vehicle is. For controllers established based on a SMC algorithm, a “chattering” problem will appear. This problem causes signals of the oscillation to be continuously noisy. Therefore, the average value of the oscillation can be increased. This only happens for the single SMC method for an electronic suspension system. Meanwhile, an OSMCPID algorithm can eliminate this

phenomenon if the controller's parameters are selected optimally. This is considered an important advantage of this new algorithm.

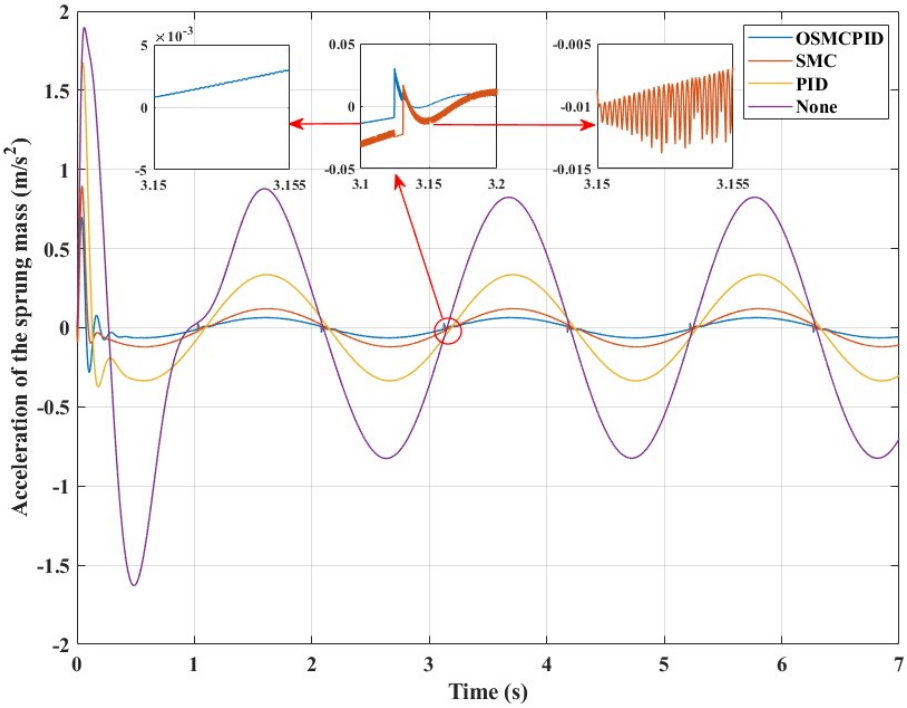

Figure 3.3. Sprung mass acceleration (The first case).

The second case:

In the following case, the pavement bump is random. This form of excitation has a very high frequency, so the smoothness of the vehicle may be affected more than in the previous case. The change of vehicle body displacement is continuous and does not follow any rules, as demonstrated in Figure 3.4. Peak values of a vehicle body displacement corresponding to four situations is 6.62 mm, 12.24 mm, 31.53 mm, and 100.43 mm, respectively. The difference between the first and fourth situations can be up to 15.17 times. This is a huge difference. In this case, the RMS criteria can also be used to evaluate oscillations over a continuous time. The average value of the oscillation is 2.38 mm, 4.42 mm, 12.04 mm, and 34.19 mm. If mean displacement values of the last situation are taken as a fixed point, the remaining values are 6.96%, 12.93%, and 35.21%, respectively. Just using the advanced suspension system, automobile's oscillation can be better improved. This efficiency can be further enhanced once the OSMCPID algorithm is utilized in order to control an active suspension system.

Acceleration values of an automotive body in the second case are more significant than in the first case. A graph in Figure 3.5 explains this. In Figure 3.5, the change of acceleration is continuous and random. Peak and average acceleration values once the vehicle only has a mechanical suspension system are 8.60 m/s^2 and 2.81 m/s^2. This value can be reduced slightly to only 7.44 m/s^2 and 2.80 m/s^2 if an automobile utilizes an active hydraulic suspension directed by a PID controller. The difference in values between these two situations is relatively small. Because this is a nonlinear oscillation, the PID algorithm's efficiency for the suspension system is not high. As mentioned in the first section, the SMC algorithm is more suitable for nonlinear systems. Peak value and average value of the automotive body acceleration are decreased to 6.11 m/s^2 and 2.01 m/s^2 if the SMC controller is utilized to direct the suspension system. Once the SMC and PID algorithms are combined, it becomes a hybrid algorithm. The hybrid algorithm with optimally selected parameters is called OSMCPID. This is the new algorithm that is used in this article. The control system's performance will be much better if a controller is built based on this new method. The maximum and average values of the oscillation have decreased sharply, to only 5.69 m/s^2

and 1.89 m/s^2. In addition, the "chattering" phenomenon does not exist when using the new hybrid algorithm. Meanwhile, this phenomenon still occurs if the controller is only established based on a single SMC algorithm. This helps to demonstrate that the quality of the OSMCPID algorithm is higher than that of a single SMC or PID algorithm.

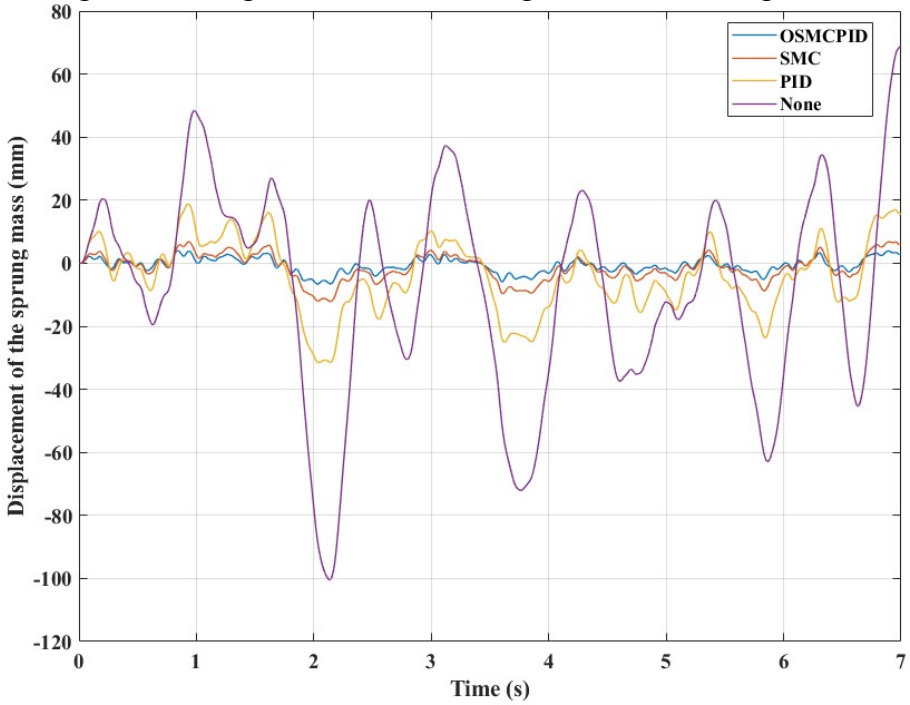

Figure 3.4. Sprung mass displacement (The second case).

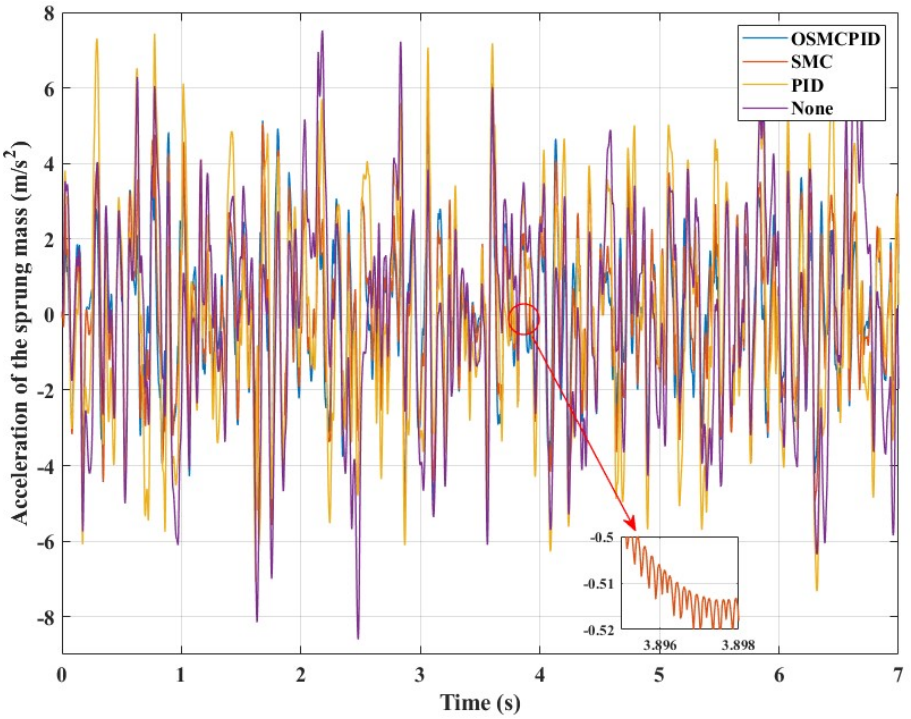

Figure 3.5. Sprung mass acceleration (The second case).

The third case:

In the last case, bump on the road takes the shape of a double step. The amplitude of the stimulus will change in three steps. Therefore, the sprung mass displacement will change by three steps. This change is shown in Figure 3.6. According to simulation results, the automotive displacement will decrease in order of None, PID, SMC, and OSMCPID. This order is valid for both steps of the oscillation. Since the time t = 6 s, the excitation signal

ends, and the displacement of the vehicle body will tend to return to zero. However, this value will fluctuate around zero for a short period before finally becoming zero. The oscillation amplitude is minimal once the OSMCPID algorithm controls the active suspension. In the other three situations, the amplitude of the oscillation is larger. Therefore, the novel hybrid algorithm will help the vehicle quickly return to a steady state after the stimulation from the road surface has ended.

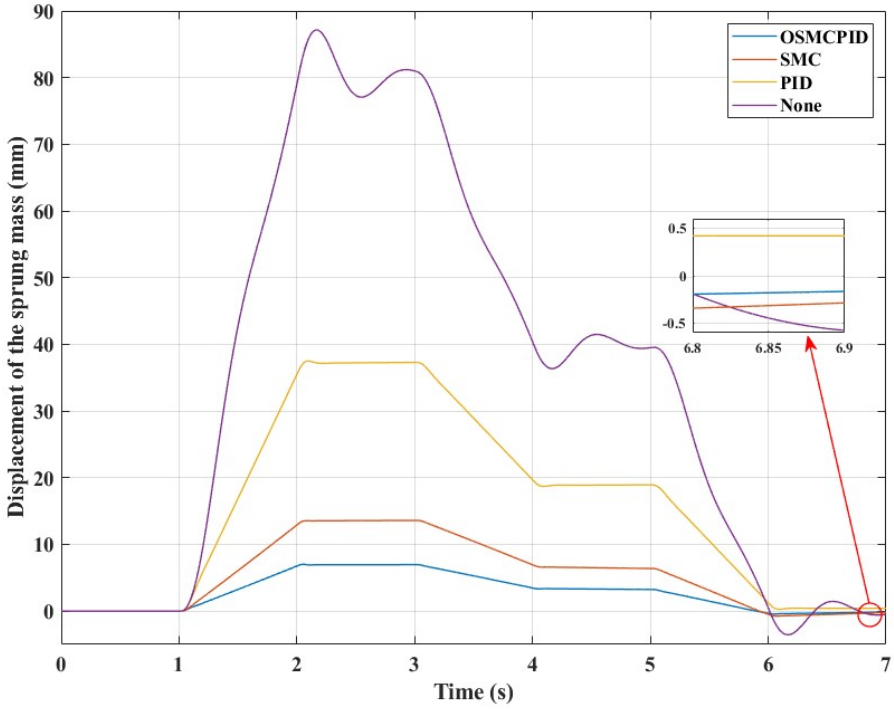

Figure 3.6. Sprung mass displacement (The third case).

In this situation, the acceleration of the vehicle's body also varies with each step of the excitation signal. The highest and lowest values of the automotive acceleration still belong to two situations: automobile utilizing a mechanical suspension system and automobile utilizing a hydraulic suspension directed by the OSMCPID method, reaching 0.64 m/s^2 and 0.23 m/s^2. The chattering phenomenon still occurs once the SMC controller is utilized to control the suspension system. Meanwhile, this phenomenon does not exist if the novel hybrid algorithm is used (Figure 3.7). This is a harmful phenomenon, and it can harm vehicle oscillation. Thanks to the new algorithm, the automobile's comfort and stability have been increased.

The values obtained from the simulation and calculation process are illustrated in Table 3.2.

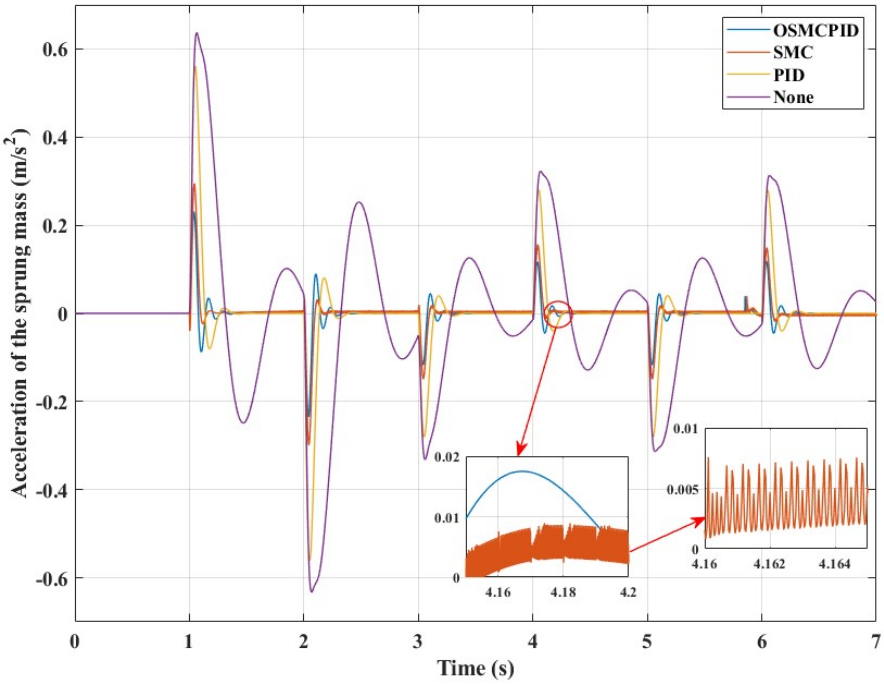

Figure 3.7. Sprung mass acceleration (The third case).

Table 3.2. Simulation results.

	Average displacement (mm)	Maximum displacement (mm)	Average acceleration (m/s^2)	Maximum acceleration (m/s^2)
	The first case			
OSMCPID	5.04	7.12	0.07	0.69
SMC	9.78	13.84	0.11	0.91
PID	26.50	37.30	0.28	1.68
None	65.36	101.00	0.68	1.90
	The second case			
OSMCPID	2.38	6.62	1.89	5.69
SMC	4.42	12.24	2.01	6.11
PID	12.04	31.53	2.80	7.44
None	34.19	100.43	2.81	8.60
	The third case			
OSMCPID	4.21	7.01	0.03	0.23
SMC	8.22	13.60	0.04	0.30
PID	22.89	37.50	0.10	0.56
None	49.47	87.16	0.19	0.64

5. CONCLUSION

Roughness on the road is the main causing of vehicle oscillation. These oscillations are able to affect negatively the comfort and smoothness of an automobile when travelling on different conditions. Suspension systems are fitted to the automobile to regulate and suppress these oscillations. Once the mechanical suspension is combined with the hydraulic actuator, it becomes an active suspension system (electronic suspension). An electronic suspension brings better quality than a mechanical suspension system.

In this article, the author has proposed a novel hybrid control algorithm called OSMCPID. This is an integrated algorithm. The final control signal is synthesized from two component algorithms, SMC and PID. The controller factors are optimally selected based on the vehicle's smoothness and stability considerations. Simulation is performed to evaluate the controller's performance. Three cases were examined; in each case, four situations were

mentioned. The input of the simulation problem is the bumpy signals of the road, and the output is the change in the automotive body's displacement and acceleration.

According to simulation results, both displacement and acceleration values are reduced when an active hydraulic suspension is used. The peak and mean values of two values above reach the minimum once the OSMCPID method is utilized to direct a suspension system. Besides, the "chattering" phenomenon did not occur when using this new hybrid algorithm. Vehicle smoothness and stability have increased dramatically.

The efficiency of the novel hybrid method, which is established in this article, has been determined through simulation. However, there is still a problem: the acceleration signal overshoots during phase transition. This problem can be improved by adding the fuzzy algorithm to this original algorithm. In addition, some experimental processes also should be performed in the future to evaluate this control algorithm's performance accurately.

REFERENCES

[1] Marenkov, I. G., & Baurova, N. I. (2021). Resistance of the Nonmetallic Air Suspension Elements of Cars to Negative Temperatures, *Russian Metallurgy*, **2021**(13), 1809–1813. doi: 10.1134/S0036029521130152

[2] Eskandary, P. K., Khajepour, A., Wong, A., & Ansari, M. (2016). Analysis and Optimization of air suspension system with independent height and stiffness tuning, *International Journal of Automotive Technology*, **17**(5), 807–816. doi: 10.1007/s12239-016-0079-9

[3] Sreenivasan G. P., & Keppanan, M. M. (2019). Analytical approach for the design of convoluted air suspension and experimental validation, *Acta Mechanica Sinica*, **35**, 1093–1103. doi: 10.1007/s10409-019-00880-z

[4] Hou, S., & Liu, G. (2020). Research on theoretical modeling and parameter sensitivity of a single-rod double-cylinder and double-coil magnetorheological damper, *Mathematical Problems in Engineering*. doi: 10.1155/2020/5489896

[5] Floreán-Aquino, K. H., et al. (2021). Modern semi-active control schemes for a suspension with MR actuator for vibration attenuation, *Actuator*, **10**(2). doi: 10.3390/act10020022

[6] Tseng, H. E., & Hrovat, D. (2015). State of the art survey: active and semi-active suspension control, *Vehicle System Dynamics*, **53**(7), 1034–1062. doi: 10.1080/00423114.2015.1037313

[7] Göhrle, C., Schindler, A., Wagner, A., & Sawodny, O. (2014). Design and Vehicle Implementation of Preview Active Suspension Controllers, *IEEE Transactions on Control Systems Technology*, **22**(3), 1135–1142. doi: 10.1109/TCST.2013.2272342

[8] Renn, J. C., & Wu, T. H. (2007). Modeling and control of a new 1/4T servo-hydraulic vehicle active suspension system, *Journal of Marine Science and Technology*, **15**(3), 265–272. doi: 10.51400/2709-6998.2400

[9] Xiao, L., Wang, M., Zhang, B., & Zhong, Z. (2020). Vehicle roll stability control with active roll-resistant electro-hydraulic suspension, *Frontiers of Mechanical Engineering*, **15**(1), 43–54. doi: 10.1007/s11465-019-0547-9

[10] Wu, Z., Li, D., & Xue, Y. (2019). A new PID controller design with constraints on relative delay margin for first-order plus dead-time systems, *Processes*, **7**(10). doi: 10.3390/pr7100713

[11] Han, S. Y., Dong, J. F., Zhou, J., & Chen, Y. H. (2022). Adaptive fuzzy PID control strategy for vehicle active suspension based on road evaluation, *Electronics*, **11**(6). doi: 10.3390/electronics11060921

[12] Demir, O., Keskin, I., & Cetin, S. (2012). Modeling and control of a nonlinear half-vehicle suspension system: a hybrid fuzzy logic approach, *Nonlinear Dynamics*, **67**, 2139–2151. doi: 10.1007/s11071-011-0135-y

[13] Khairuddin, S. H., Hasan, M. H., Hashmani, M. A., & Azam, M. H. (2021). Generating clustering-based interval fuzzy type-2 triangular and trapezoidal membership functions: a structured literature review, *Symmetry*, **13**(2). doi: 10.3390/sym13020239

[14] Ho, C. M., Nguyen, C. H., & Ahn, K. K. (2022). Adaptive fuzzy observer control for half-car active suspension systems with prescribed performance and actuator fault, *Electronics*, **11**(11). doi: 10.3390/electronics11111733

[15] Chen, X. W., & Zhou, Y. (2018). Modelling and analysis of automobile vibration system based on fuzzy theory under different road excitation information, *Complexity*. doi: 10.1155/2018/2381568

[16] Dangor, M., Dahunsi, O. A., Pedro, J. O., & Ali, M. M. (2014). Evolutionary algorithm-based PID controller tuning for nonlinear quarter-car electrohydraulic vehicle suspensions, *Nonlinear Dynamics*, **78**, 2795–2810. doi: 10.1007/s11071-014-1626-4

[17] Liu, J., et al. (2019). Modeling and Simulation of Energy-Regenerative Active Suspension Based on BP Neural Network PID Control, *Shock and Vibration*. doi: 10.1155/2019/4609754

[18] Pedro, J. O., Nhlapo, S. M. S., & Mpanza, L. J. (2020). Model predictive control of half-car active suspension systems using particle swarm optimisation, *IFAC PapersOnline*, **53**(2), 14438–14443. doi: 10.1016/j.ifacol.2020.12.1443

[19] Manna, S., et al. (2022). Ant colony optimization tuned closed-loop optimal control intended for vehicle active suspension system, *IEEE Access*, **10**, 53735–53745. doi: 10.1109/ACCESS.2022.3164522

[20] Zhou, Y., Chen, S., & Wang, J. (2014). Two-acceleration-error-input proportional-integral-derivative control for vehicle active suspension, *Journal of Traffic and Transportation Engineering*, **1**(3), 228–234. doi: 10.1016/S2095-7564(15)30106-9

[21] Nguyen, T. A. (2021). Improving the comfort of the vehicle based on using the active suspension system controlled by the double-integrated controller, *Shock and Vibration*. doi: 10.1155/2021/1426003

[22] Nguyen, M. L., et al. (2022). Application of MIMO control algorithm for active suspension system: a new model with 5 state variables, *Latin American Journal of Solids and Structures*, **19**(2). doi: 10.1590/1679-78256992

[23] Park, M., & Yim, S. (2021). Design of static output feedback and structured controllers for active suspension with quarter-car model, *Energies*, **14**(24). doi: 10.3390/en14248231

[24] Kaleemullah, M., Faris, W. F., Rashid, M. M., and Hasbullah, F. (2021). Comparative analysis of LQR and robust controller for active suspension, *International Journal of Vehicle Noise and Vibration*, 8(4), 367-386. DOI: 10.1504/IJVNV.2012.051541

[25] Haddar, M., et al. (2021). Intelligent optimal controller design applied to quarter car model based on non-asymptotic observer for improved vehicle dynamics, *Proceedings of the Institution of Mechanical Engineers, Part I: Journal of Systems and Control Engineering*, 235(6), 929-942. DOI: 10.1177/0959651820958831

[26] Ho, C. M., Tran, D. T., & Ahn, K. K. (2021). Adaptive sliding mode control based nonlinear disturbance observer for active suspension with pneumatic spring," *Journal of Sound and Vibration*, **509**. doi: 10.1016/j.jsv.2021.116241

[27] Ovalle, L., Ríos, H., & Ahmed, H. (2022). Robust control for an active suspension system via continuous sliding-mode controllers, *Engineering Science and Technology, an International Journal*, **28**. doi: 10.1016/j.jestch.2021.06.006

[28] Nguyen, T. A. (2021). Advance the efficiency of an active suspension system by the sliding mode control algorithm with five state variables, *IEEE Access*, **9**, 164368–164378. doi: 10.1109/ACCESS.2021.3134990

[29] Wang, Z., et al. (2022). Suspension system control based on type-2 fuzzy sliding mode technique, *Complexity*. doi: 10.1155/2022/2685573

[30] Nguyen, D. N., Nguyen, T. A., & Dang, N. D. (2022). A novel sliding mode control algorithm for an active suspension system considering with the hydraulic actuator, *Latin American Journal of Solids and Structure*s, **19**(1). doi: 10.1590/1679-78256883

[31] Toyoma, S., & Ikeda, F. (2015). Integral sliding mode control for active suspension systems of half-vehicle model, *Mechanical Engineering Journal*, **2**(3). doi: 10.1299/mej.14-00550

[32] Zhao, F., et al. (2015). Adaptive neural-sliding mode control of active suspension system for camera stabilization, *Shock and Vibration*. doi: 10.1155/2015/542364

[33] Łuczko, J., & Ferdek, U. (2016). Continuous and discrete sliding mode control of an active car suspension system, *Journal of Theoretical and Applied Mechanics*, **54**(1), 3–11. doi: 10.15632/jtam-pl.54.1.3

[34] Moghadam, A. R., & Kebriaei, H. (2019). Stochastic sliding mode control of active vehicle suspension with mismatched uncertainty and multiplicative perturbations, *Asian Journal of Control*, **22**(6), 2330–2339. doi: 10.1002/asjc.2135

[35] Lin, B., Su, X., & Li, X. (2019). Fuzzy sliding mode control for active suspension system with proportional differential sliding mode observer, *Asian Journal of Control*, **21**(1), 1–13. doi: 10.1002/asjc.1882

[36] Qin, Y., et al. (2018). Suspension hybrid control for in-wheel motor driven electric vehicle with dynamic vibration absorbing structures, *IFAC-PapersOnline*, **51**(31), 973–978. doi: 10.1016/j.ifacol.2018.10.054

[37] Mahmoodabadi M. J., & Javanbakht, M. (2020). Optimum Design of an Adaptive Fuzzy Controller as Active Suspension for a Quarter-Car Model, *IETE Journal of Research*. doi: 10.1080/03772063.2020.1772129

[38] Zhou, C., et al. (2018). Optimal sliding mode control for an active suspension system based on a genetic algorithm, *Algorithms*, **11**(12). doi: 10.3390/a11120205

[39] Zahra, A. K. A., & Abdalla, T. Y. (2020). Design of fuzzy super twisting sliding mode control scheme for unknown full vehicle active suspension systems using an artificial bee colony optimization algorithm, *Asian Journal of Control*, **23**(4), 1966–1981. doi: 10.1002/asjc.2352

